

CFD modelling of large scale liquid hydrogen experiments indoors and outdoors

S.G. Giannisi^{1*} and A.G.Venetsanos¹

¹ *Environmental Research Laboratory, National Center for Scientific Research Demokritos, Aghia Paraskevi, Athens, 15341, Greece, sgiannisi@ipta.demokritos.gr, venets@ipta.demokritos.gr*

ABSTRACT

The use of liquid hydrogen in maritime applications is expected to grow in the coming years, in order to meet the decarbonisation goals that EU countries and countries worldwide have set for 2050. In this context, The Norwegian Public Roads Administration commissioned large-scale LH2 dispersion and explosion experiments both indoors and outdoors, which were conducted by DNG GL in 2019 to better understand safety aspects of LH2 in the maritime sector. In this work, the DNV unignited outdoor and indoor tests have been simulated and compared with the experiments with the aim to validate the ADREA-HF Computational Fluid Dynamics (CFD) code in maritime applications. Three tests, two outdoors and one indoors, were chosen for the validation. The outdoor tests (test 5 and 6) involved liquid hydrogen release vertically downwards and horizontal to simulate an accidental leakage during bunkering. The indoor test (test 9) involved liquid hydrogen release inside a closed room to simulate an accident inside a tank connection space (TCS) connected to a ventilation mast.

Keywords: two-phase, CFD, safety, ADREA-HF, bunkering, liquefied hydrogen

1.0 INTRODUCTION

The use of liquid hydrogen in maritime sector is expected to grow in the coming years, in order to meet the decarbonisation goals that EU countries and countries worldwide have set for 2050. The behaviour of hydrogen dispersion in case of an accidental liquid spill has been studied in the past with the help of both experimental and numerical studies. However, there are more limited studies related to LH2 spills compared to compressed hydrogen releases.

The best-known large-scale LH2 experiments that can be used for CFD validation purposes include: the NASA series [1] consisted of seven large-scale experiments with 5.7 m³ LH2 spilled with release rates up to 10-15 kg/s; the BAM experiments [2] with four LH2 pool spill tests aiming to study pool spread on water and on an aluminium sheet. The release rate was ranged at around 5-6 L/s LH2 (~300 g/s); the HSL 2010 series [3] with LH2 spill tests both at elevation and at ground level in open environment subject to wind variability and the HSE 2020 series [4], which was a new experimental series of LH2 spill experiments in the same facility as in the HSL 2010 series and with release rates up to 350 g/s.

In all experiments, a common feature was that the cloud initially exhibited a dense behaviour, but at some distance from the release as it absorbs heat from the environment and the ground it becomes buoyant and is lifted of the ground. A visible cloud is formed due to humidity condensation and HSL 2010 and HSE 2020 experiments revealed that close to the release point air also freezes.

In the past, several numerical studies have simulated LH2 spills and several CFD codes and modelling approaches have been validated against some of the above experiments. A non-exhaustive review of relevant numerical studies is presented next.

The NASA experiments have been simulated in [5]-[10]. Different CFD codes and modelling approaches were employed by the different scientific teams and different parameters were analysed. In the work of Venetsanos and Bartzis 2007 [5] the source is treated with two different approaches: 1)

* Current affiliation: Motor Oil, 12A Irodou Attikou Str.151 24, Maroussi, Greece, sgiannisi@moh.gr

evaporating pool where only vapour enters the CFD domain and 2) two-phase jet, where hydrogen in vapour and liquid phase enters the CFD domain. The phase distribution inside the domain is computed using the Raoult's law for ideal mixtures. The two-phase jet gave better predictions. Middha et al. 2011[9] used a coupled model with pool spreading and evaporating modelling and vapour dispersion modelling. The liquid pool was modelled using the shallow water model. The evaporated from the pool hydrogen entered the CFD domain, where only vapour hydrogen existed. The results showed that this coupled model was efficient for the investigation of complex accidental release scenarios of cryogenic liquids. In [8], the effect of humidity on liquid hydrogen spills was investigated using modified expressions of Lee model to account for the phase changes of water and hydrogen. The simulation results that modelled the air humidity were more consistent with the experiment. Similar conclusion was extracted also in Giannissi et al. [6]. In the same work a parametric study testing different levels of humidity showed that humidity makes the cloud more buoyant and the higher the humidity level the higher the effect was. This in turn led to reduction of the LFL distance on ground. In [7], the effect of other factors, like ambient temperature, wind speed and ground temperature, on vapour dispersion was investigated by simulated the NA6 experiment. The main conclusions were that the thermal interaction between ground-cloud plays significant role in the LH2 release and affects the overall behaviour of the mixture. The increased wind speed tended to expand the downwind distance of the flammable cloud, despite the decreasing of the time for full diffusion and the increased wind temperature seemed to delay the hydrogen diffusion due to the increased air viscosity. Lastly, Holborn et al. [10] used the FLACS CFD code to simulate large-scale liquid hydrogen pool releases based on the NASA experiments. The computational results were qualitatively similar to the experimental results, but quantitative there were significant differences. In the same study using the FLACS simulations the hazardous distances were predicted for several spill rates, in order to provide data for future safety analyses in LH2 aircraft and airport LH2 storage facilities.

BAM experiments have been simulated by [9], [11] and [12]. In [9], the FLACS CFD code was used and tested the under development then pool model (see also previous paragraph). The simulations predicted the maximum concentrations within a factor of two for each of the BAM sensors. More than a decade earlier Schmidt et al. [11] and Statharas et al. [12] simulated also the BAM experiments. In [12], it was concluded that given all the uncertainties, like complicated wind patterns, back flow of the plume near the source, etc., the applied model was in reasonable agreement with the experiment with the maximum concentrations to be predicted within a factor of two in most cases. Schmidt et al. [11] concluded that the CFD model they used was suitable for estimation of the dispersion of gaseous hydrogen, however the agreement with the experiment was not the desired one and this was partially attributed to the limited amount of data collected due to disadvantageous meteorological conditions.

The HSL 2010 experiments have been simulated by Ichard et al. [13], who examined the air components condensation effect using the Homogeneous Equilibrium Model (HEM) model. The predictions showed that the air condensation had an effect on the vertical spill test and not much on the horizontal spill test. Giannissi et al. has also simulated the HSL 2010 tests in [14] and [15]. The main conclusion of both studies is that humidity and air phase change can affect the dispersion of the mixture in LH2 releases and the modelling approach plays significant role in the capability of the code to accurately reproduce the physical phenomena. A non-homogeneous model which accounts for the slip velocity of the non-vapour phase improved the predictions. However, it was highlighted that the model that is used to calculate the slip velocity and the assumed droplet/particle diameter greatly affects the results and needs special treatment to avoid unphysical predictions.

The HSL 2020 experiments were simulated by Giannissi et al. [16] using two CFD codes, the FLACS and ADREA-HF, and their results were compared with the measurements. The comparison showed that both simulations were within a factor of 2 for most of the sensors in terms of concentration and temperature predictions. The computational results were closer to the field measurements near to the release point, whereas the tendency to diverge from the experimental data (over-prediction) was observed at longer distances. This was partially explained by the fluctuation of the wind direction.

Finally, we should also mention that Gitushi et al. 2023 [19] have published a numerical work related to LH2 spills inside a shock tube to mimic a spill inside a tunnel. These simulations have been performed to assist the experimental design of LH2 experiments inside confined space. These experiments are anticipated to provide useful input for models validation. The simulations showed that the height and length of the flammable plume is highly dependent on the wind, and any confinement of the pool on the ground will result in a taller plume.

The Norwegian Public Roads Administration commissioned large-scale LH2 dispersion and explosion experiments both indoors and outdoors, which were conducted by DNG GL in 2019 [17] to better understand safety aspects of LH2 in the maritime sector. To the authors' knowledge this is the first experimental work with LH2 release inside closed space under more controlled ambient conditions. The experiments have been simulated by Hansen and Hansen 2022 [18]. The predictions were in satisfactory agreement with the experiment indicating that the dispersion resulting for LH2 release can be predicted with reasonable confidence using the CFD methodology.

In this work, two outdoor tests, test 5 and test 6, and one indoor test, test 9, from the recent DNV experimental series [17] are simulated with the aim to validate the ADREA-HF CFD code. Test 5 involves a vertically downwards release from a 10 barg tanker in open environment exposed to naturally varying wind, while Test 6 is a horizontal release from a 10 barg in the same facility. In test 9, liquid hydrogen is released vertically downwards from 10 barg inside a container with a ventilation mast.

2.0 OVERVIEW OF THE LH2 EXPERIMENTS

The Norwegian Public Roads Administration commissioned seven outdoor release experiments and eight indoor release experiments with the aim to contribute to the understanding of the LH2 behaviour for its introduction in maritime applications as a fuel [17]. The release rates in the tests were representative of releases that could occur during bunkering operations. Some of the tests were also ignited to study flame propagation and pressure generation, but measurements during the dispersion are available for these tests too.

For the current work, two outdoor experiments, test 5 (vertical release) and test 6 (horizontal release), and one indoor experiment, test 9, were selected for the simulations. Table 1 is an overview of the selected experiments, whereas in the next Sections a brief description is presented.

Table 1. Summary of the conditions for the experiments that were selected for simulations.

| | Initial tanker pressure (barg) | Release direction | Nozzle diameter (mm) | Mass flow rate (kg/min) | Release duration (s) | Ambient temperature (°C) | Mean wind speed (m/s) | Mean wind direction (degrees) |
|---------------|--------------------------------|---------------------------|----------------------|-------------------------|----------------------|--------------------------|-----------------------|-------------------------------|
| Test 5 | 10 | 0.32 m vertical downwards | 25 | 42.9 | 120 | 3.7 | 5.2 | 257 |
| Test 6 | 10 | 0.5 m horizontal | 25 | 49.9 | 120 | 3.8 | 2.7 | 245 |
| Test 9 | 10 | 0.32 m vertical downwards | 25 | 32.6 | 660 | 2.8 | 2.8 | 151 |

2.1 Outdoor experiments

LH2 was released either horizontally in line with the average wind (0.5 m height) or vertically downwards (0.32 m height) above a concrete through a 25 mm (1 inch) nozzle. The LH2 tanker pressure varied between 0.8-10 barg and thus the mass flow rate was ranged from 9.7-49.9 kg/min. In the test field two ISO containers (one on top of the other) were positioned to simulate the ship's side. In addition, a barrel and other obstacles were placed on the test pad.

The ambient temperature was 3-4°C. Variant wind with mean speed ranged from 3.2-6.7 m/s (based on one high sensor at 10 m and one low sensor at 5 m) was measured during the experiments. The mean wind direction in most of the tests was approximately WS^\dagger , except for test 2 where E wind direction was measured and thus the arrangement of the concentration sensors and the thermocouples in test 2 was different from the rest tests.

In the experiments, pad temperature, field temperature and gas concentration, were recorded. The pad and field temperatures were measured with thermocouples. The gas concentration was measured with oxygen sensors. The pad temperature was measured on the surface of the concrete pad at distances of 0.2, 0.5, 1.0, 5.0 and 10.0 m from the release point. In addition, measurements were taken at 20 mm and 30 mm depth inside the concrete at several distances from the release point. Totally 48 thermocouples were placed on or in the concrete test pad. The field temperature and gas concentration sensors were deployed at rows of 30, 50 and 100 m distance from the release point, at heights of 0.1, 1.0 and 1.8 m above the ground (Figure 1, left). The field temperature was also measured at ground level (0 m). Totally 40 thermocouples were used for field temperature measurements and 30 oxygen sensors for gas measurements. More details and figures with the instrumentation setup can be found in [17].

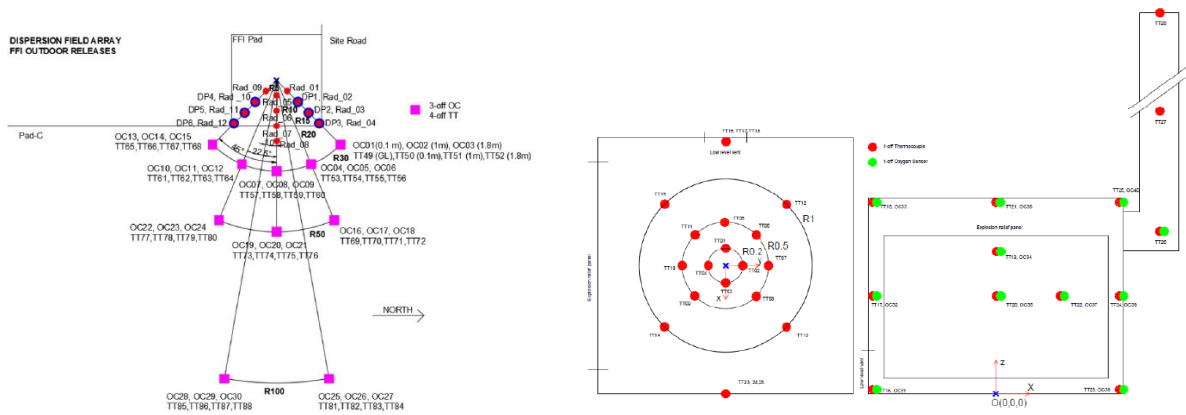


Figure 1. Sensor locations for measurements of temperature (TT) and gas concentration (OC) in test 5 and 6 (left) and test 9 (right) [17].

2.2 Indoor experiments

The indoor experiments were conducted to simulate spill in tank connection space (TCS) connected to a ventilation mast. Leakage of LH2 in an enclosed space is of special interest as there is limited documentation and experimental on this topic. The release is assumed to occur inside the TCS. TCS are normally filled with tubes, pipelines, valves, processing equipment etc., which can affect the hydrogen dispersion and the propagation of a deflagration detonation transition. Hence, the TCS used in most of tests (except for test 8 and test 9) contained structures to mimic these lines and tubes.

The release was vertically downwards at 0.32 m height in all indoor tests through a 25 and 12 mm (1 and ½ inch) nozzle. The initial LH2 tanker pressure was ranged from 1.5-10 barg (only the first indoor test, test 8, had a low pressure of 1.5 barg and the rest tests were at 10 barg) and the spill rate was 11-40.1 kg/min. The TCS had internal dimensions H2.26 x W2.96 x D2.69 m. The ventilation mast had a horizontal length of 3 m, a 90 ° bend, and a vertical length of 10.025 m. Its diameter was 0.450 m. At the opposite from the ventilation mast wall there was a lower level vent, which in some tests was sealed. In test 9 it was open.

[†] A W wind direction would be in line with the release.

The ambient temperature was 3-9oC. The wind direction was S and SW in most of the tests and the mean wind speed was ranged from 2.3-5.9 m/s. In test 9, which was selected for simulation the wind direction was SSE.

Thermocouples and oxygen sensors were placed inside the TCS at several distances from the release and different heights (see Figure 1, right) and outside the TCS. The location of the sensors outside the TCS varied between the first indoor test (test 8) and the rest tests, as it was observed that hydrogen was not dispersed at long distances downwind the TCS. Thus, the final arrangement includes sensors across rows at 30 and 50 m from the release at several heights and sensors in front of the ISO containers. In addition, three thermocouples were placed along the ventilation mast at three different heights. More details and figures with the instrumentation setup can be found in [17].

3.0 MODELING STRATEGY

3.1 Methodology

For the simulations the ADREA-HF CFD code is used, which solves the 3D time-dependent conservation equations of mass, momentum and enthalpy for the mixture. The conservation equation of hydrogen total mass fraction (vapour and liquid) is also solved. The phase distribution in each cell is computed assuming equilibrium using the Raoult's law. For the turbulence the k-ε model with extra buoyancy terms is used. More details about the methodology and the equations can be found in [15].

In the present study the ambient humidity is neglected and the air was modelled as one component (with mass-weighted properties based on its composition in nitrogen and oxygen), which cannot undergo through any phase change. The significance of modelling the humidity and air phase change in LH2 spills has been highlighted in [15]. However, this approach increases considerably the complexity of the problem and the run time of the simulations. Thus, initially we run the simplified simulations neglecting the humidity and air phase change and as follow-up of this work we will perform additional simulations taking into account these parameters too.

The source is modelled as a two-phase jet. The conditions at the source were calculated by performing isentropic expansion from 2.25 barg (measured pressure upstream the orifice) to ambient pressure and then calculating the velocity at the orifice from the measured mass flow rate and the orifice area. Table 2 shows the conditions that were used as hydrogen input for the simulations.

Table 2. Source data for the simulations.

| | Velocity (m/s) | Pressure (Pa) | Temperature (K) | Vapour volume fraction | Liquid mass fraction |
|---------------|----------------|---------------|-----------------|------------------------|----------------------|
| Test 5 | 135.25 | 101325 | 20.35 | 0.86 | 0.895 |
| Test 6 | 157.32 | 101325 | 20.35 | 0.86 | 0.895 |
| Test 9 | 102.78 | 101325 | 20.35 | 0.86 | 0.895 |

In the horizontal releases the upwind numerical scheme is used for the discretization of convective terms of all variables. In the vertical releases the MUSCL scheme (high order numerical scheme) is applied in all variables, except for the turbulent kinetic energy and the turbulent dissipation rate, where the upwind scheme is used. The different treatment in vertical releases is based on (Tolias and Venetsanos 2015) findings [20], where they suggest to avoid using first order schemes for the discretization of the convective terms in vertical releases, as they can lead to an unphysical phenomenon, the “butterfly” phenomenon. Hence, higher order schemes, such as MUSCL were recommended. For the discretization of the diffusive terms the central differences scheme is used and for the time integration the fully implicit 1st order scheme is applied in all simulations.

3.2 Domain, grid and boundary conditions

3.2.1 Outdoor releases

The domain is extended in all directions (Figure 2) with the longitudinal direction (x-axis downwind the source) to be extended more. The source is located at (0,0) and at the respective height based on the simulated test, e.g. at 0.32 m for test 5. The grid for test 5 consists of 660 660 cells and for test 6 of 690 060 cells. The smallest cell is equal to the size of the source and encloses the source (i.e., 1 cell is used to discretize the source). The grid is then extended in all directions with small expansion ratios up to 1.12.

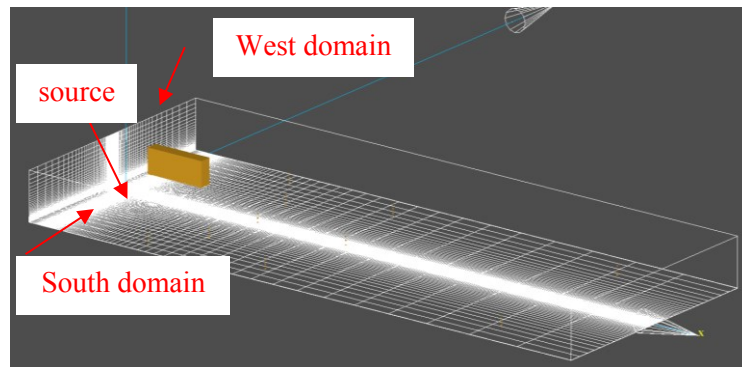


Figure 2. The grid on the bottom and west domain for test 5. The ISO containers and the sensors are also visible. Similar domain and grid was used for the test 6 too.

The containers that were set as obstacles in the experiments were modelled as one box of total height equal to the height of the two containers one on top of the other. Since, no data were available for the containers' dimensions the ISO standards for shipping containers were used. More specifically, ISO 40 ft containers were assumed, i.e. 12.19m long x 2.44m wide x 2.59m. The rest small obstacles in the test pad were neglected due to lack of details for their exact dimensions and position.

In both outdoor tests the wind was with a direction almost W (SW). Based on the release orientation in the experiment this corresponds to a wind blowing from the west and south boundary in the CFD domain of Figure 2. Thus, both west and south boundaries are set as wind inlet boundaries. First, a 3D problem without release is solved with given value for u - and v - component of the velocity (w -component is assumed zero) according the experimental wind conditions to obtain the wind field in the entire domain. The steady state solution of the 3D problem without release is used as initial and boundary condition for the 3D dispersion problem.

The ground is treated as solid boundary. The ground temperature is updated at every time step by solving 1D temperature equation inside the underground to account for heat flux from the ground. Concrete material is used for the ground. At all open boundaries the constant pressure boundary condition is imposed except for the east domain where zero gradient is applied. For the hydrogen concentration and temperature the given value, if inflow and zero gradient if outflow condition was applied at all boundaries except for the wind boundaries and the source boundary.

3.2.2 Indoor releases

The ventilation mast was modelled as a rectangular with the same open area as the experimental mast, in order to be aligned with the grid lines of the Cartesian grid[‡]. Both the vent opening and the low-level opening were discretized with more than 2 cells in each of their cross-section dimensions to allow for both outflow and inflow of the mixture. One cell was used to discretize the source. The

[‡] ADREA-HF code designs Cartesian grid.

domain was extended in all directions around the container and the vent mast. In total, 464 448 cells were used.

The wind was with a direction E. Thus, the east boundary is set as wind inlet boundary. Similar to the outdoor test simulations, a 3D problem without release is solved with given value for u- component of the velocity (v- and w-components are assumed zero) according to the experimental wind conditions to obtain the wind field in the entire domain. The steady state solution of the 3D problem without release is used as initial and boundary condition for the 3D dispersion problem.

At the all open boundaries the zero gradient boundary conditions is applied except for the top boundary where the constant pressure boundary conditions is imposed. For the hydrogen concentration and temperature, however, at all boundaries except for the wind boundaries and the source boundary the given value, if inflow and zero gradient if outflow condition was applied. Heat fluxes from the solid boundaries, e.g. the TCS floor, are accounted by solving a 1D temperature equation inside the solid substrate.

4.0 RESULTS AND DISCUSSION

4.1 Outdoor releases

4.1.1 Vertical release - Test 5

Figure 3 (left) shows the hydrogen concentration contour plot on the ground level at steady state for the simulation. The cloud is shifted away from the release centreline due to the wind direction. Further downwind the release (after about 30 m) the cloud heats up due to the air entrainment and the ground heat flux and becomes buoyant. Hence, concentrations on ground level are below half-LFL (2% v/v) 50 m downwind the release point. The buoyant behaviour of the cloud is also confirmed by the shape of Lower Flammability Limit (LFL) iso-surface (4 % v/v) illustrated in Figure 3 (right).

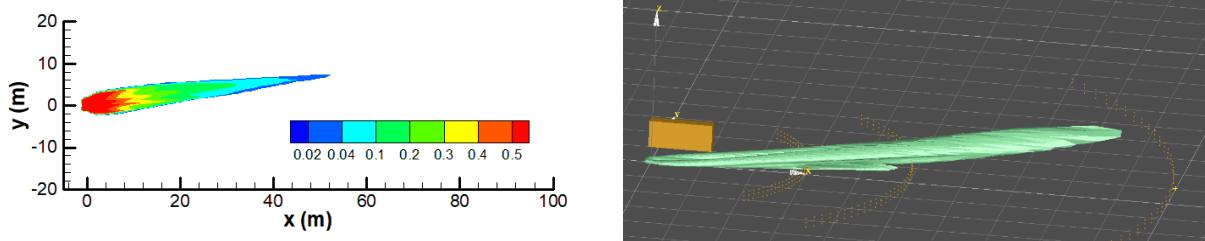


Figure 3. Steady state H₂ concentration contours on ground level (left) and the LFL iso-surface cloud (right) at steady state for test 5.

The predicted cloud is narrow in the transverse direction (along y-axis) and drifted towards the dominated (average) wind direction. This results in very low predicted concentrations at all experimental sensors. In the experiment the measurements indicate a wider cloud, because the peak hydrogen concentrations ($\sim 7.5\%$ v/v) were measured at the sensors 22.5° from the release centreline at the row 30 m and heights 1 and 1.8 m, but concentrations above the half-LFL were also measured at the sensors along the release centreline at 30 m.

Due to wind variability concentrations above half-LFL were measured for short duration at the sensors opposite to the average wind direction, while at the same time the concentrations at the sensors along the wind direction were reduced to almost zero. For example, in Figure 4 we can observe that the concentration at sensors OC_11 (light green line) located 22.5° from the release centreline measured a peak concentration at the time when the concentration at OC_5 (purple line) was reduced almost to

zero before increasing again. Thus, wind variability and different turbulence levels can explain the different behaviour between observed and predicted cloud.

Figure 5 shows the maximum concentration of simulation versus the experiment. The maximum concentration is over predicted at row 30 m at all heights except for 1 m height, where the prediction is in excellent agreement with the experiment. At row 50 m the concentration is in fairly good agreement with the experiment with a tendency to over predict it.

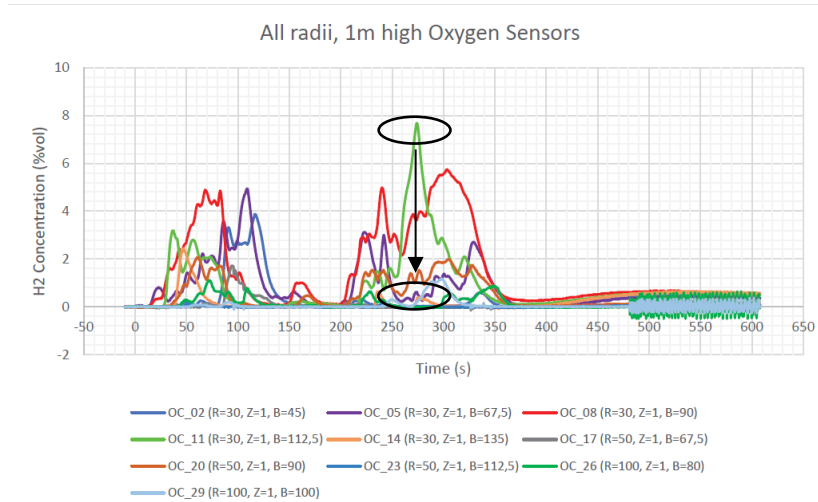


Figure 4. Chart with gas measurements taken from [17]. A preliminary test was conducted at 0 sec. The actual test 5 initiated at around 200 sec.

The highest maximum concentrations in Test 5 were 6.2 to 7.7% v/v, measured at the sensors 30 m from the release, in 22.5° angle relative to the release orientation and at different heights. At 1 and 1.8 m heights the measured concentrations were the highest. In the simulation, the highest concentration at row=30 m was at 1.8 m with the concentration at 0.1 m to follow. The significant higher concentrations predicted at 1.8 m height indicate a more buoyant cloud in the simulations.

Based on the data given in [17] the experimental field temperatures ranged from 264.65 to 277.25 K, while in the simulations ranged from 244 to 277 K with the lowest temperature measured and predicted at row=30 m (see Figure 5, right). The temperature at 50 m and 100 m were close to ambient in both the experiment and the simulation, indicating that liquid hydrogen didn't reach these areas. This is also confirmed with the low concentrations observed at row=50 m (see Figure 5, left). The lowest temperatures at row=30 m, were generally predicted at the greater heights in the simulation, i.e. 1 m and 1.8 m. This is in line with what was observed in the experiment. However, the temperature at 1.8 m height was under predicted. This behaviour is in line with the findings based on the concentration measurements.

In the experiment, liquid hydrogen was observed on the surface at 0.2 m and 0.5 m from the release point based on the pad temperature measurements. The code can provide a rough estimate of the liquid pool size by making the assumption that if liquid hydrogen is predicted in the cells adjacent to the ground then a pool is formed over the entire area of these cells. Based on this approach, the simulation predicted a liquid pool of approximately 0.75 m radius, even though the shape of the pool was not exactly circular.

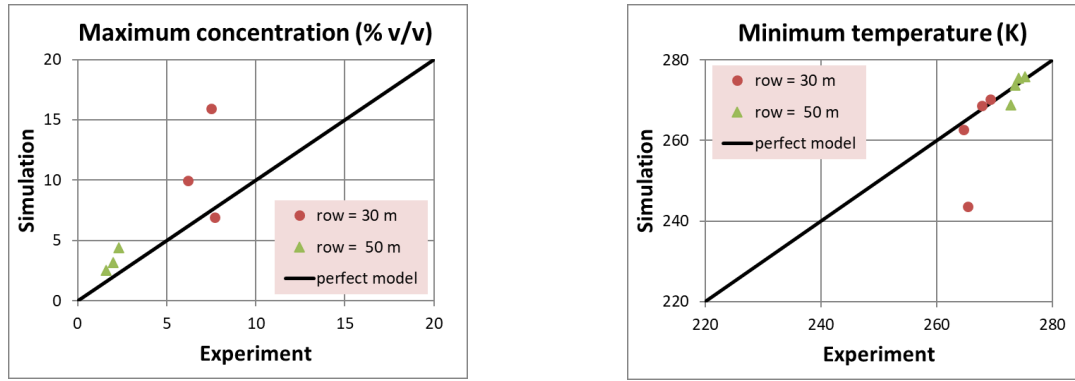


Figure 5. Experiment versus simulation for test 5: maximum H₂ concentration (left) and minimum temperature (right) across the row 30 and 50 m. A perfect model would lie along the black solid line.

4.1.2 Horizontal release - Test 6

Figure 6 (left) shows the steady state H₂ concentration contour plot on the ground level as predicted by the simulation. The effect of wind direction is apparent, as the mixture is shifted at an angle relative to the release similar to the angle of the wind direction. Figure 6 (right) presents the 4% v/v iso-surface of hydrogen at steady state. The buoyant behaviour of the cloud approximately 20 m downwind the release point can be observed.

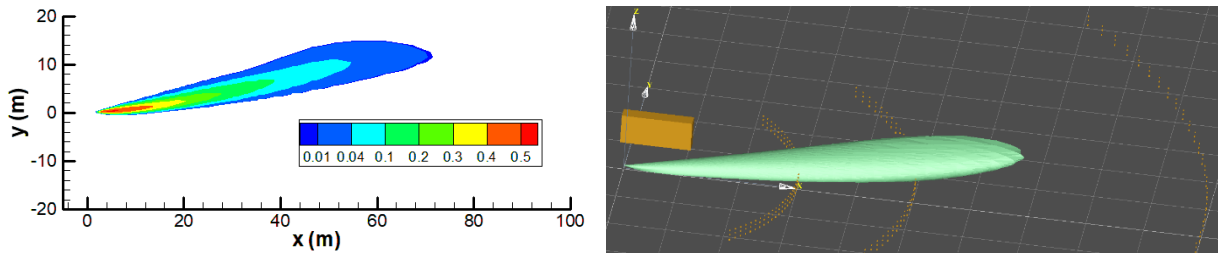


Figure 6. Steady state H₂ concentration contours on ground level (left) and the LFL iso-surface cloud (right) for test 6. The sensors are also depicted.

Based on the sensor output the cloud in the experiment should be wider. Two high concentrations (21 and 15.6 % v/v) were measured at row 30 m and 0.1 m height in two sensors (sensor OC_04 and OC_07), which are located at different from the release angles by 22.5° (about 10 m distance in the y-axis). In the simulations the cloud is narrower and its concentration half-width[§] is about 1.7 m at row 30 m. Similar to test 5 these discrepancies can be attributed to wind variability and different levels of turbulence between simulation and experiment.

The maximum concentration is well predicted at 30 m and seriously over predicted at 50 m, as shown in Figure 7. This is also in line with the fact that in simulations we have less mixing and jet spreading and the cloud travels further downwind along the wind direction.

Based on the data given in [17] the experimental field temperatures ranged from 247.45 to 277 K (see also Figure 7). The lowest temperatures were measured at the sensors closest to the release point (30 m), both in line with and 22.5° angle relative to the release centreline (orientation). The temperatures measured at the other sensors were similar to ambient temperature, indicating that liquid hydrogen didn't reach these areas. In the simulation the lowest temperature was 238 K predicted at the sensor at row 30 m and height 1 m.

[§] The transverse distance from the jet centerline to the point where the concentration is half of the centerline concentration (volume fraction)

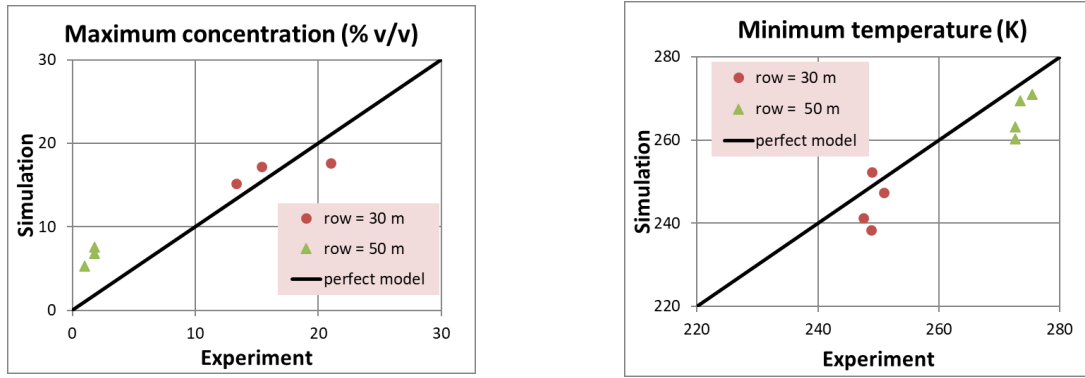


Figure 7. Experiment versus simulation for test 6: maximum H₂ concentration (left) and minimum temperature (right) across the row 30 and 50 m. A perfect model would lie along the black solid line.

Finally, the simulation didn't predict any liquid pool on the ground similar to what was observed in the experiment based on the pad temperature.

4.2 Indoor release

4.2.1 Vertical release - Test 9

Figure 8 presents the hydrogen volume fraction (right) and temperature contours (middle) at steady state for the indoor test 9. The TCS is saturated with hydrogen almost immediately after the start of the release. In around 30 sec the concentration of hydrogen was 99% v/v. Similar, behaviour was observed in the experiment too [17].

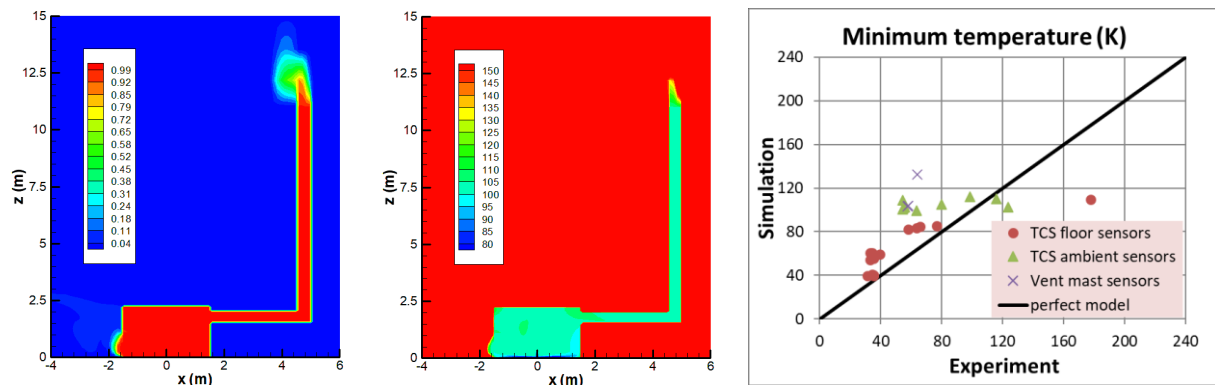


Figure 8. Hydrogen volume fraction (left) and temperature contours (middle) at steady state, and the minimum temperature for sensors inside the TCS and the vent mast for simulation versus experiment**.

Figure 8 (right) shows the minimum measured temperature compared to minimum predicted temperature for the sensors inside the TCS and the vent mast. In the experiment the lowest temperatures were 32 K, measured on the floor at 0.2 and 0.5 m from the release. Higher temperatures were measured on the floor 1.0 m from the release ranging from 58-77 K. The lowest ambient temperature inside the TCS was 54 K measured at several points (see in [17]) and the temperature inside the vent mast was around 58 K with no significant drop throughout its length. In the simulation the temperatures are in fairly good agreement with the experiment with a tendency for over-prediction

** Floor sensors are the sensors on the TCS floor, ambient sensors are the sensors inside the TCS container and vent mast sensors are the sensors along the ventilation mast.

at all sensors except for the close to the low-level vent sensor (T16) and two sensors on the TCS ceiling (T21 and T25). However, the highest vent sensor seriously over-predicts the temperature.

Liquid hydrogen was predicted on the TCS floor in a circular area of approximately 0.2 m diameter. Similarly, in the experiment based on the temperatures liquid hydrogen was observed on the floor at around 0.2 m from the release.

According to the field temperature measurements and the concentration measurements no cold hydrogen was spread far from the vent mast. However, near the low-level vent outside the TCS a maximum concentration equal to 66% v/v was detected indicating that hydrogen exited the TCS through this opening. This was also supported by the temperature measurements. In the simulation, a similar behaviour was predicted as shown in Figure 8. However, higher concentrations up to 99 % were predicted close to the low-level opening.

Simulations with adiabatic TCS floor were also tested and showed that modelling the ground heat flux is significant in LH2 releases. Without the increased buoyancy and acceleration due to the heat absorbed from the floor the mixture did not have the sufficient momentum to travel through the entire vertical section of the vent mast and exit the vent. After few seconds the outside air entered from the top and pushed hydrogen back. This is a quite interesting remark and should be further investigated to exclude any numerical/modelling issues that might generate this phenomenon.

5.0 CONCLUSIONS

The recent LH2 spill experiments commenced by the Norwegian Public Roads Administration have been simulated in this work using the CFD methodology and the ADREA-HF code. A horizontal outdoor, a vertical outdoor and a vertical indoor test have been simulated.

In the outdoor vertical test, the maximum concentrations were generally over predicted. Good agreement was found at the sensors at the row 50 m and excellent agreement with the experiment was found at the sensor at row 30 m and 1 m height. Generally, fairly good agreement between measured and predicted temperature. In the outdoor horizontal test the predictions were in satisfactory agreement with the experiment in terms of the maximum concentration levels at row 30 and 50 m. However, the simulation tends to over predict the maximum concentration in this test too. In the horizontal spill test no liquid pool was formed based on the simulation and the experimental data. On the contrary, in the vertical spill test a small liquid pool close to the release was observed in the experiment according to the pad temperature readings and was also predicted by the simulations.

Given the uncertainties in presence of variable wind in the outdoor tests the performance of the CFD simulations was satisfactory. The least agreement of the vertical test with the experiment reveals that the vertical spills are more complex due to phenomena that occur because of the greater interaction with the ground.

The indoor vertical test predicted the minimum temperature inside the TCS room with fairly good agreement at most sensors with a tendency for over-prediction. The temperatures in the ventilation mast were also well predicted, except from the sensor closer to the vent exit, where the temperature was significantly over-estimated. Based on a sensitivity study heat fluxes from solid boundaries are very significant in LH2 releases and should be modelled.

Future simulations will include modelling the phase change of nitrogen, oxygen and humidity, in order to contribute to the understanding of the underlying phenomena, like the unwanted inflow of oxygen into TCS due to negative pressure or the clogging of ventilation mast due to solidification of moisture in the atmosphere.

Acknowledgments

ELVHYS project No. 101101381 is supported by the Clean Hydrogen Partnership and its members. UK participants in Horizon Europe Project ELVHYS are supported by UKRI grant numbers 10063519 (University of Ulster) and 10070592 (Health and Safety Executive). Funded by the European Union. Views and opinions expressed are however those of the author(s) only and do not necessarily reflect those of the European Union or the Clean Hydrogen Partnership. Neither the European Union nor the Clean Hydrogen Partnership can be held responsible for them.

REFERENCES

- [1] J. Witcofski, RD, Chirivella, “Experimental and analytical analyses of the mechanisms governing the dispersion of flammable clouds formed by liquid hydrogen spills,” *Int. J. Hydrogen Energy*, vol. 9, no. 5, pp. 425–435, 1984.
- [2] S. B. Marinescu-Pasoi L, “Messung der Ausbreitung einer Wasserstoff- und Propangaswolke in bebautem Gelände und Gasspezifische Ausbreitungsversuche, Battelle Ingenieurtechnik GmbH. Reports R-68.202 and R-68.264,” 1994.
- [3] P. Hooker, D. B. Willoughby, and M. Royle, “Experimental releases of liquid hydrogen,” in *4th Int. Conf. on Hydrogen Safety*, 2011, vol. San Franci, p. paper 160.
- [4] J. Hall *et al.*, “Characterisation, dispersion and electrostatic hazards of liquid hydrogen for the PRESLHY project,” in *9th International Conference on Hydrogen Safety, Edinburgh, UK, September 21-23, 2021*.
- [5] A. Venetsanos and J. Bartzis, “CFD modeling of large-scale LH2 spills in open environment,” *Int. J. Hydrogen Energy*, vol. 32, no. 13, pp. 2171–2177, Sep. 2007.
- [6] S. G. Giannissi, A. G. Venetsanos, G. Momferatos, and N. Markatos, “Modeling the humidity phase change in large scale liquid hydrogen spills,” in *International Conference on Energy, Environment and Storage of Energy*, 2020.
- [7] T. Jin, M. Wu, Y. Liu, G. Lei, H. Chen, and Y. Lan, “CFD modeling and analysis of the influence factors of liquid hydrogen spills in open environment,” *Int. J. Hydrogen Energy*, vol. 42, no. 1, pp. 732–739, 2017.
- [8] Y. Liu *et al.*, “Modeling the development of hydrogen vapor cloud considering the presence of air humidity,” *Int. J. Hydrogen Energy*, vol. 44, no. 3, pp. 2059–2068, 2019.
- [9] P. Middha, M. Ichard, and B. J. Arntzen, “Validation of CFD modelling of LH2 spread and evaporation against large-scale spill experiments,” *Int. J. Hydrogen Energy*, vol. 36, no. 3, pp. 2620–2627, Feb. 2011.
- [10] P. G. Holborn, C. M. Benson, and J. M. Ingram, “Modelling hazardous distances for large-scale liquid hydrogen pool releases,” *Int. J. Hydrogen Energy*, vol. 45, no. 43, pp. 23851–23871, 2020.
- [11] U. Schmidt, D., Krause, U., Schmidtchen, “Numerical simulation of hydrogen gas releases between buildings,” *Int. J. Hydrogen Energy*, vol. 24, no. 5, pp. 479–488, May 1999.
- [12] J. C. Statharas, A. G. Venetsanos, J. G. Bartzis, J. Würtz, and U. Schmidtchen, “Analysis of data from spilling experiments performed with liquid hydrogen,” *J. Hazard. Mater.*, vol. 77, no. 1–3, pp. 57–75, Oct. 2000.
- [13] M. Ichard, O. R. Hansen, P. Middha, and D. Willoughby, “CFD computations of liquid hydrogen releases,” *Int. J. Hydrogen Energy*, vol. 37, no. 22, pp. 17380–17389, Nov. 2012.
- [14] S. G. Giannissi, A. G. Venetsanos, N. Markatos, and J. G. Bartzis, “CFD modeling of hydrogen dispersion under cryogenic release conditions,” *Int. J. Hydrogen Energy*, vol. 39, no. 28, pp. 15851–15863, Sep. 2014.
- [15] S. G. Giannissi and A. G. Venetsanos, “Study of key parameters in modeling liquid hydrogen release and dispersion in open environment,” *Int. J. Hydrogen Energy*, vol. 43, no. 1, pp. 455–467, 2018.
- [16] S. G. Giannissi, A. G. Venetsanos, E. Vyazmina, S. Jallais, S. Coldrick, and K. Lyons, “CFD simulations of large scale LH2 dispersion in open environment,” in *9th International Conference on hydrogen safety, 21-24 September, online, 2021*.

- [17] J. Aaneby, T. Gjesdal, and Ø. Voie, “Large scale leakage of liquid hydrogen (LH2) – tests related to bunkering and maritime use of liquid hydrogen,” 2021.
- [18] O. R. Hansen and E. S. Hansen, “CFD-modelling of Large-scale LH2 Release Experiments,” *Chem. Eng. Trans.*, vol. 90, no. May, pp. 619–624, 2022.
- [19] K. Mangala Gitushi, M. Blaylock, and E. S. Hecht, “Simulations for Planning of Liquid Hydrogen Spill Test,” *Energies*, vol. 16, no. 4, 2023.
- [20] I. C. Toliás and A. G. Venetsanos, “Comparison of Convective Schemes in Hydrogen Impinging Jet CFD Simulation,” in *6th International Conference on Hydrogen Safety (ICHHS 2015), Yokohama, Japan, 19-21 October, 2015*.